



LJMU Research Online

Stansfield, BN, Brown, AD, Stewart, CE and Burniston, JG

Dynamic Profiling of Protein Mole Synthesis Rates During C2C12 Myoblast Differentiation

<http://researchonline.ljmu.ac.uk/id/eprint/13860/>

Article

Citation (please note it is advisable to refer to the publisher's version if you intend to cite from this work)

Stansfield, BN, Brown, AD, Stewart, CE and Burniston, JG (2020) Dynamic Profiling of Protein Mole Synthesis Rates During C2C12 Myoblast Differentiation. Proteomics. ISSN 1615-9853

LJMU has developed [LJMU Research Online](#) for users to access the research output of the University more effectively. Copyright © and Moral Rights for the papers on this site are retained by the individual authors and/or other copyright owners. Users may download and/or print one copy of any article(s) in LJMU Research Online to facilitate their private study or for non-commercial research. You may not engage in further distribution of the material or use it for any profit-making activities or any commercial gain.

The version presented here may differ from the published version or from the version of the record. Please see the repository URL above for details on accessing the published version and note that access may require a subscription.

For more information please contact researchonline@ljmu.ac.uk

<http://researchonline.ljmu.ac.uk/>

1 Dynamic profiling of protein mole synthesis rates during C2C12 myoblast
2 differentiation.

3 **Running title: Protein synthesis during myoblast differentiation**

4 Ben N. Stansfield*, Alexander D. Brown*, Claire E. Stewart, and Jatin G. Burniston†.

5 Research Institute for Sport & Exercise Sciences, Liverpool John Moores University, Liverpool, UK.

6 *These authors contributed equally to the work.

7 †Address for Correspondence: Jatin G Burniston PhD FECSS
8 Professor of Muscle Proteomics
9 Research Institute for Sport & Exercise Sciences (RISES)
10 Liverpool Centre for Cardiovascular Science (LCCS)
11 Liverpool John Moores University,
12 Tom Reilly Building, Byrom Street,
13 Liverpool, L3 3AF,
14 United Kingdom.
15 Tel: +44 (0) 151 904 6265
16 Email: j.burniston@ljmu.ac.uk

17

18 **Keywords:**

19 Deuterium oxide; Fractional synthesis rate; Mass spectrometry; Protein synthesis; Stable isotope

20 **Word Count**

21 5079 including references and figure legends

22 Abstract

23 Mole (MSR) and fractional (FSR) synthesis rates of proteins during C2C12 myoblast differentiation were
24 investigated. Myoblast cultures supplemented with D₂O during 0-24 h or 72-96 h of differentiation were
25 analysed by LC-MS/MS to calculate protein FSR and MSR after samples were spiked with yeast alcohol
26 dehydrogenase (ADH1). Profiling of 153 proteins detected 70 significant ($p \leq 0.05$, FDR $\leq 1\%$)
27 differences in abundance between cell states. Early differentiation was enriched by clusters of
28 ribosomal and heat shock proteins, whereas later differentiation was associated with actin filament
29 binding. The median (first - third quartile) FSR (%/h) during early differentiation 4.1 (2.7-5.3) was ~2-
30 fold greater than later differentiation 1.7 (1.0-2.2), equating to MSR of 0.64, (0.38-1.2) and 0.28, (0.1-
31 0.5) fmol/h/ug total protein, respectively. MSR corresponded more closely with abundance data and
32 highlighted proteins associated with glycolytic processes and intermediate filament protein binding
33 that were not evident amongst FSR data. Similarly, MSR during early differentiation accounted for 78
34 % of the variation in protein abundance during later differentiation, whereas FSR accounted for 4%.
35 Conclusively, the interpretation of protein synthesis data differed when reported in mole or fractional
36 terms, which has consequences when studying the allocation of cellular resources.

37 **Statement of Significance**

38 Fractional protein synthesis measurements may be confounded when studying systems undergoing
39 changes in protein abundance. To address this issue, we further developed our dynamic proteome
40 profiling (DPP) method to include protein abundance (ABD) data measured in mole units against a
41 spiked-in standard (yeast alcohol dehydrogenase 1). When combined with fractional synthesis rates,
42 measured by mass isotopomer analysis, ABD data enable the calculation of mole synthesis rates (MSR)
43 on a protein-by-protein basis. During C2C12 differentiation MSR and FSR data gave rise to different
44 biological interpretations. MSR measurements during early differentiation prediction subsequent
45 changes in protein abundance better than FSR and exhibited a stronger relationship with published
46 changes in RNA.

47

48 1. Introduction

49 Muscle primarily consists of multinucleated myofibers, that originate from myogenic precursors
50 through a program of differentiation during embryonic development^[1]. Myogenic differentiation is also
51 reactivated during regeneration in adult muscle, in response to injury or during periods of adaptation
52 to exercise^[2]. The differentiation of myogenic precursors involves complex temporal patterns of gene
53 expression^[3] and cell cycle regulation^[4]. However, differentiation also involves substantial changes to
54 the myocyte proteome^[5] and during differentiation myoblasts fuse and hypertrophy, which may be
55 accompanied by changes to the synthesis of individual proteins. Targeted analyses^[6] report the
56 synthesis of contractile proteins coincides with myoblast fusion but wider-spread changes in protein
57 abundance occur during the differentiation program^{[5] [7]}, including changes to proteins specifically
58 involved in ribosomal translation^[8].

59 Stable isotope labelling of amino acids in cell culture (SILAC), has allowed for measurements of
60 individual protein fractional synthesis rates (FSR) in C2C12 myotubes^[9]. More recently deuterium oxide
61 (D₂O) labelling has been adopted to investigate mixed protein FSR in C2C12 myoblasts and myotubes
62^[10, 11]. We have studied protein-specific FSR in rat^[12, 13] and human^{[14] [15]} muscle using D₂O *in vivo* and
63 dynamic proteome profiling (DPP)^[16] to study both the relative abundance and FSR of individual
64 proteins. However, FSR data are fractional measurements of an unknown whole, i.e. protein
65 abundance. Therefore, the interpretation of FSR may be confounded when used to study changes in
66 cell state underpinned by marked changes in protein abundance^[5]. Co-occurring changes in protein
67 abundance may need to be incorporated with synthesis data to gain an accurate interpretation
68 biological processes^{[17] [18]}. Herein we report a development of our DPP method to provide synthesis
69 and data in mole (e.g. fmol/h/ug total protein) units. Importantly, the biological interpretation of our
70 current data is different when expressed in mole rather than fractional terms, and our data expressed
71 in mole units gave a better prediction of subsequent changes in protein abundance.

72 2. Materials and Methods

73 2.1 Cell Culture

74 C2C12 murine myoblasts (ATCC; Rockville, MD, USA) were resuscitated from liquid nitrogen and seeded
75 onto gelatinised T75 flasks (Nunc, Roskilde, Denmark) at 1×10^6 cells/ml in growth medium (GM)
76 containing: Dulbecco's Modified Eagle Medium (DMEM), 10 % heat-inactivated fetal bovine serum
77 (FBS), 10 % heat-inactivated new-born calf serum, 2 mM L-glutamine, and 1 % penicillin-streptomycin.
78 Cells were incubated in 5 % CO₂ at 37 °C (HERAcell 150i incubator; Thermo Scientific) until 80 %
79 confluent and then reseeded at 100,000 cells/ml on gelatinised 6-well plates (Nunc, Roskilde,
80 Denmark).

81 Upon attaining 80 % confluency, cells were washed twice in phosphate buffered saline (PBS; 10 mM
82 phosphate buffer, 2.7 mM KCL, 137 mM NaCl, pH 7.4; Sigma-Aldrich, Dorset, UK) and incubated in 2 ml
83 differentiation medium (DM) containing: DMEM, 2 % heat-inactivated horse serum, 2 mM L-glutamine,
84 1 % penicillin-streptomycin. Isotopic labelling of newly synthesised proteins was achieved by
85 supplementing DM with sterilised 99.8 % D₂O (Sigma-Aldrich, Dorset, UK). To investigate protein FSR
86 during early differentiation, separate cultures of cells were incubated in DM containing either H₂O or
87 D₂O during 0 h – 24 h of differentiation. Similarly, protein FSR during late differentiation was
88 investigated in separate cell cultures incubated in DM containing either H₂O or D₂O during 72 h – 96 h
89 of differentiation. Proteins extracted from control (DM + H₂O) cells were used to measure the natural
90 isotopic abundance of proteins in the absence of D₂O. Cell photomicrographs were acquired after 0 h
91 and 96 h of culture in DM (Figure 1) and analysed using Image J software (IBIDI, Munich, Germany).
92 Myotubes were classified as cells that contained 3 or more myonuclei/tube. Myotube length (μm) was
93 measured along the long axis of each myotube, diameter (μm) was averaged from measurements at
94 three equidistant positions, and myotube area (μm^2) was calculated by drawing manually around the
95 sarcolemma.

96 2.2 Proteomic analysis

97 Cells were washed twice with ice cold PBS, prior to incubation on ice in 250 μ l/well RIPA buffer (0.5 M
98 Tris-HCL, pH 7.4, 1.5 M NaCl, 2.5 % deoxycholic acid, 10 % NP-40, 10 mM EDTA) for 5 min. Cells were
99 then harvested using a cell scraper and stored at -80 °C. The protein concentration of harvested
100 samples was measured using a bicinchoninic acid (BCA™) protein assay (Pierce, Rockford, IL) against
101 bovine serum albumin (BSA) standards (0-2 mg/ml) prepared in RIPA buffer. Proteins were digested
102 consistent with our recent work ^[13-15]. Briefly, lysates containing 100 μ g protein were digested with
103 trypsin using the filter aided sample preparation (FASP) method. Aliquots, containing 4 μ g peptides,
104 were desalted using C₁₈ Zip-tips (Millipore, Billerica, MA, USA) and resuspended in 0.1 % formic acid
105 spiked with 10 fmol/ μ l yeast alcohol dehydrogenase (ADH1) (Waters Corp. Milford, MA) in preparation
106 for liquid chromatography-mass spectrometry (LC-MS/MS) analysis.

107 Peptide mixtures were analysed by nanoscale reverse-phase ultra-performance liquid chromatography
108 (UPLC; NanoAcquity; Waters Corp.) and online electrospray ionization quadrupole–time-of flight mass
109 spectrometry (Q-TOF Premier; Waters Corp.), as previously reported ^[13-15]. For all measurements, the
110 mass spectrometer was operated in positive electrospray ionization mode at a resolution of $>10,000$
111 full width at half maximum (FWHM). Peptide mass spectra were recorded between 350 and 1600 m/z
112 using survey scans of 0.9 s duration with an interscan delay of 0.1 s. In addition, data-dependent MS/MS
113 spectra were collected from control samples over the range 50–2000 m/z for the 5 most abundant
114 precursor ions of charge 2+ or 3+. The mass spectrometry proteomics data have been deposited to
115 ProteomeXchange (<http://www.proteomexchange.org>), dataset identifier PXD021125.

116 2.3 Label-free quantitation of protein abundance

117 Label-free quantitation was performed using Progenesis Quantitative Informatics for proteomics
118 (Nonlinear Dynamics, Newcastle, UK) consistent with our previous work ^[13, 14, 19]. MS/MS spectra were
119 exported in Mascot generic format and searched against the Swiss-Prot database restricted to ‘mus

120 musculus' (17,006 sequences) using a locally implemented Mascot (www.matrixscience.com) server
121 (version 2.2.03). The enzyme specificity was trypsin allowing 1 missed cleavage, carbamidomethyl
122 modification of cysteine (fixed), deamidation of asparagine and glutamine (variable), oxidation of
123 methionine (variable) and an m/z error of ± 0.3 Da. The Mascot output (xml format), restricted to non-
124 homologous protein identifications was recombined with MS profile data in Progenesis. For statistical
125 analysis, log-transformed MS data were normalized by inter-sample abundance ratio, and differences
126 in relative protein abundance were investigated using nonconflicting peptides only. In addition, data
127 were normalised to yeast ADH1 to estimate protein abundances in fmol/ μ g protein using the Hi-N
128 method ^[20].

129 2.4 Calculation of protein synthesis rates

130 Peptide mass isotopomer abundance data were extracted from MS only spectra using Progenesis
131 Quantitative Informatics (Nonlinear Dynamics, Newcastle, UK). Consistent with our previous work <sup>[13-
132 15]</sup>, the abundances of the monoisotopic peak (m_0), m_1 , m_2 and m_3 mass isotopomers were collected
133 over the entire chromatographic peak for each non-conflicting peptide that was used for label-free
134 quantitation. Peptides that were not resolved to at least 4 mass isotopomers (m_{0-3}) were excluded.

135 Precursor enrichment was back calculated from peptide mass isotopomer data according to ^[12, 21].
136 Briefly the enriched molar fraction of each mass isotopomer was calculated by subtracting the molar
137 fraction of the unlabelled control peptide from the equivalent D₂O-labelled peptide and the enrichment
138 ratio between m_2 and m_1 mass isotopomers was used to calculate precursor enrichment (p) using
139 equation 1.

$$140 \quad p = \left(\left(\frac{EM_2}{EM_1} \right) / \frac{(n-1)}{2} \right) \cdot 100$$

141 (Equation 1)

142 Where EM_1 is the enriched molar fraction of m_1 and EM_2 is the enriched molar fraction of m_2 and n is
143 the number of H-D exchange sites counted by referencing the peptide amino acid sequence against
144 standard tables ^[22].

145 Incorporation of deuterium into newly synthesized protein results in a decrease in the molar fraction
146 (fm_0) of the monoisotopic (m_0) peak that follows the pattern of an exponential decay. The rate constant
147 (k) for the decay of fm_0 was calculated as a first-order exponential spanning from the beginning (t_0) to
148 end (t) of the 24 h D_2O labelling period.

$$149 \quad k = \frac{1}{t - t_0} \cdot -\ln\left(\frac{fm_{0t}}{fm_{0t_0}}\right)$$

150 (Equation 2)

151 The rate of change, k , is a function of the number (n) of 2H exchangeable H—C bonds, and this was
152 accounted for by referencing each peptide sequence against standard tables ^[22]. FSR, was derived by
153 dividing k by the molar percent enrichment of deuterium in the precursor (p) pool. Protein FSR was
154 reported as the median of peptide values assigned to each protein (decimal values were multiplied by
155 100 to give FSR in (%/h). Protein half-life ($t_{1/2}$) in h was estimated from decimal FSR data by Equation 3:

$$156 \quad t_{1/2}^1 = \frac{\ln 2}{\left(\frac{FSR}{100}\right)}$$

157 (Equation 3)

158 Mole synthesis rate (MSR) was calculated by multiplying protein FSR expressed as a decimal by the
159 protein abundance normalised to the 50 fmol yeast ADH1 spike-in^[20].

160 2.5 Statistical analysis

161 Statistical analyses were performed in R Studio version 3.6.2. Data are presented as mean \pm SD unless
162 otherwise stated. Morphological analysis of control and labelled myotubes after 96 h differentiation
163 was conducted using independent t-tests. Data collected from cell cultures harvested at 0 h and 24 h

164 (control and labelled) of differentiation were used to quantify protein abundances (n = 3) during early
165 differentiation. Similarly, control and labelled cultures harvested at 72 h and 96 h were used to provide
166 abundance measurements (n=3) during later differentiation. Differences in protein abundance
167 between early and later differentiation were investigated by ANOVA. Statistical significance was set at
168 $p \leq 0.05$ and FDR was set at 1 % based on q values ^[23]. Data from each H₂O (control) and D₂O labelled
169 sample were used to calculate protein FSR and MSR during early (24 h) or late (96 h) differentiation.

170 2.6 Bioinformatics

171 2D enrichment analysis ^[24] was conducted against published ^[25] transcriptome data, using the Perseus
172 platform ^[26], with significance being set at $p \leq 0.02$. Protein interactions were investigating using
173 bibliometric mining in the search tool for the retrieval of interacting genes/proteins (STRING;
174 <http://string-db.org/>) ^[27].

175 3. Results and Discussion

176 Supplementation of DM with D₂O had no observable effect on myocyte differentiation (Figure 1B and
177 C). There were equivalent numbers of myotubes in n=3 fields of view in control (14 ± 3) and deuterium-
178 labelled (13 ± 3) cells. Myotube length (60.03 ± 22.51 μm) and diameter (6.5 ± 2.37 μm) in deuterium-
179 labelled cultures was not different from the length (59.53 ± 24.88 μm) and diameter (6.03 ± 1.99 μm)
180 of myotubes grown in control DM (Figure 1D-F). As expected, the distribution of peptide mass
181 isotopomers was similar between samples harvested prior to (Figure 1G) and after (Figure 1H) 24 h
182 incubation in control DM, whereas cells grown in DM supplemented with D₂O exhibited robust changes
183 in isotopomer distribution and a decrease in the fraction (f_{m₀}) of the peptide monoisotopic (m₀) peak
184 (Figure 1I).

185 Label free quantitation included 3546 peptides from 153 proteins that had at least one unique peptide
186 detected in each sample during both early and later periods of differentiation. Ten proteins (n = 12
187 peptides) were not identified in all samples and were disregarded. The complete list of protein
188 abundance and synthesis data is provided in Supplementary Table 1. Seventy proteins exhibited
189 statistically significant (P ≤ 0.05, FDR ≤ 1%) differences in abundance between early and late
190 differentiation (Figure 2A), including 27 proteins that increased and 43 proteins that decreased in
191 abundance. Our current profiling of abundance data add to earlier analyses of C2C12 myoblast
192 differentiation using 2-D gel electrophoresis ^[7] and LC-MS/MS ^[5]. In agreement with earlier reports ^[5],
193 ribosomal proteins and eukaryotic initiation factors were enriched in C2C12 myoblasts. In addition,
194 proteins associated with chromatin regulation (e.g. nucleosome assembly protein; NAP1L1;^[28]), cell
195 proliferation (e.g. prothymosin alpha; PTMA ^[29]) and protein folding (e.g. peptidyl-prolyl cis-trans
196 isomerase A ;PPIA ^[30]) were significantly greater in abundance during early differentiation (Figure 2A).
197 Heat shock proteins are integral to protein translation and prevent misfolding during elongation or
198 assist in the correct folding of polypeptides after termination ^[31]. Isoforms of HS90 (HS90A, HS90B)
199 maintain proteostasis by facilitating the degradation of unfolded or redundant proteins ^[32]. We report

200 significantly greater abundance of each HS90 isoform during early differentiation, alongside
201 mitochondrial heat shock protein (CH60) that facilitates the correct folding of proteins imported to the
202 mitochondrial matrix^[33]. These findings provide the first protein confirmation of transcriptome analysis
203^[34], reporting differential expression of HSP genes during the differentiation of mouse primary
204 myoblasts.

205 2D Enrichment analysis (Figure 2B) demonstrated that differentiation was associated with significant
206 enrichment of cytoskeletal components and actin filament-based processes that were not reflected at
207 the transcriptome level. Conversely, the transcriptome data highlighted the enrichment of biosynthetic
208 process during differentiation, which were not faithfully replicated at the proteome level. The
209 disparities between RNAseq and proteome data may relate to differences in sampling time (4 d in the
210 current proteomic work and 7 d in the published^[25] RNAseq analysis) or may suggest regulation by
211 processes in addition to transcription. Indeed, the correlation between protein abundance changes and
212 published^[25] RNAseq differences at 24 h and 7 days of differentiation was $r^2=0.3275$ (Figure 2C), which
213 is similar to past publications^[35].

214 Changes in protein abundance are ultimately underpinned by the balance between protein synthesis
215 and protein degradation. Protein FSR was calculated for 115 of the 153 proteins that had clearly
216 resolved mass isotopomer envelopes in both labelled and unlabelled samples. The median FSR of
217 proteins early during differentiation (4.11, IQR = 2.70-5.31 %/h) was ~2 fold greater than the median
218 FSR (1.70, IQR = 0.97-2.16 %/h) later during differentiation. These FSR values equate to a median half-
219 life ($t_{1/2}$) of 16.9 h and 44.4 h during early and late differentiation, respectively. Cell cycle arrest occurs
220 rapidly after myoblasts are transferred to DM^[36] and the marked decrease in protein turnover is
221 consistent with the significant reduction in the abundance of ribosomal proteins (Figure 2A). Notably,
222 the average half-life of proteins during 72 – 96 h of differentiation in C2C12 (0.9 ± 0.6 d) was
223 substantially shorter than their corresponding half-life's in young mouse EDL (22.5 ± 17.2 d) or soleus
224 muscle in vivo (16.6 ± 8.8 d). There was also no relationship ($r^2 < 0.03$) amongst 32 proteins that were
225 matched in the current work with FSR reported in mouse fast- and slow-twitch muscle in vivo^[39]. These

226 findings are consistent with ^[40] and raise challenges for the integration of data across cell and animal
227 models. Our calculations and those of previous work in C2C12 myoblasts ^[11] do not incorporate cell
228 doubling time which is common practice in models such as yeast ^[37]. We cannot exclude that some
229 proliferation of myoblasts may continue in DM but the low serum conditions and high cell confluency
230 argue against an effect of proliferation substantially inflating protein FSR values particularly during early
231 differentiation. Our FSR data align well with the limited existing literature reporting either average FSR
232 of protein mixtures ^[11] or protein-specific FSR data ^{[9] [38]} in C2C12. Future studies with higher temporal
233 resolution will be required to clarify whether some proliferation continues in the hours immediately
234 after cells are transferred to DM.

235 FSR data report synthesis as a fraction of an unknown whole (i.e. protein abundance), whereas our
236 current MSR data incorporate FSR measurements with protein-specific abundance data. Linear
237 regression analyses found FSR was a minor component in the variance of MSR during either early or
238 later differentiation (Figure 3A and B, respectively). Therefore, protein abundance was the principal
239 contributing factor to the variance in MSR data, which underpins the advantage of using MSR to
240 investigate experimental scenarios where changes in abundance are expected to co-occur alongside
241 changes in synthesis rates. Indeed, the relationship between data during early and late differentiation
242 improved from $r^2=0.19$ (FSR; Figure 3C) to $r^2=0.73$ for (MSR; Figure 3D), which suggests MSR may offer
243 a greater predictive power than fractional data. Protein FSR during early differentiation also had no
244 relationship ($r^2=0.04$) with protein abundance during later differentiation (Figure 4A). In contrast,
245 protein MSR during early differentiation predicated 78 % of the variance in protein abundance at the
246 later stage of differentiation (Figure 4B). The remaining variance is likely to be accounted for by
247 degradation, which also contributes to both increases and decreases in the abundance of individual
248 proteins ^[14]. We also compared changes in mRNA expression measured by ribosomal profiling ^[25]
249 against changes in protein synthesis rates during myoblast differentiation. The relationship between
250 changes in protein synthesis and ribosomal profiling was greater when protein synthesis data was
251 expressed in mole units (Figure 4D, $r^2=0.29$) rather than fractional terms (Figure 4C, $r^2=0.11$). Moreover,

252 a number of disparities (e.g. nestin (NEST), DESM, FLNC and MYH3) between responses reported by
253 ribosomal profiling and protein synthesis measurements were resolved when protein synthesis data
254 were expressed in mole rather than fractional units.

255 MSR data generated more coherent protein interaction networks than FSR (Figure 5) and the biological
256 interpretation of the data was different when synthesis was expressed in either fractional terms (Figure
257 5A and C) or mole units (Figure 5B and D). Functional annotation of the top-ranked proteins by MSR
258 found glycolytic processes were enriched during both early (Figure 5B) and late (Figure 5D)
259 differentiation, which was not evident in the analysis of FSR data (Figure 5A and C). In addition,
260 intermediate filament organisation and myofilament protein binding were enriched amongst MSR data
261 during later differentiation. Myofibrillogenesis requires the co-ordinated synthesis of actin, myosin,
262 tropomyosin and alpha actin ^[6] and, in the current work, myoblast differentiation resulted in significant
263 increases in the abundance of sarcomeric proteins including, embryonic myosin heavy chain (MYH3),
264 essential myosin light chain (MYL1) and the fast-twitch isoform of the sarco-/endoplasmic Ca²⁺ ATPase
265 (AT2A1). Intermediate filament proteins, including desmin (DESM) and vimentin (VIM) were
266 incorporated within the MSR protein networks but were not included in the protein interaction network
267 generated from FSR data (Figure 5B). Furthermore, we detected increases in non-muscle isoforms
268 (MYH9, ML12B), which is consistent with the formation of pre-myofibrils during 72-96 h rather than
269 mature sarcomeres ^[41].

270 To the best of our knowledge, we report the first investigation of myoblast differentiation using protein-
271 specific synthesis and abundance measurements in mole rather than fractional units. Our analysis of
272 115 proteins that met stringent quality control criteria is limited compared to the breadth of analysis
273 of dynamic SILAC, which used higher resolution MS and reported half-life data for 3,528 proteins in
274 C2C12 myotubes only ^[9]. We anticipate high-resolution MS analysis of deuterium-labelled samples
275 would achieve a similar proteome coverage to dynamic SILAC and biosynthetic labelling with deuterium
276 may afford a greater sensitivity to detect differences in protein synthesis rates. Dynamic SILAC
277 experiments typically monitor the incorporation of heavy isotope at a single lysine or arginine residue

278 per peptide, whereas deuterium may be incorporated in to the majority of amino acids ^[22] and could
279 provide a proportionally greater MS signal. Whether deuterium outperforms dynamic SILAC as sample
280 complexity increases remains to be investigated and each approach suffers potentially greater risk of
281 being confounded by co-eluting peptides (e.g. compared to standard label-free quantitation) as sample
282 complexity rises. Deuterium oxide is considerably cheaper than SILAC reagents and can be used in a
283 broader range of biological systems, including humans ^[14] ^[15] and rats ^[12, 21]. Herein, we demonstrate
284 the advantages of combining deuterium labelling with methods ^[20] for estimating protein abundance
285 in mole units to provide MSR data. Dynamic proteome profiling is a robust method ^[15] and future
286 application on higher resolution instrumentation is likely to provide more comprehensive data.
287 Currently, it is unclear whether some proteins may be synthesised in excess ^[9] or whether there are
288 close relationships between protein synthesis and abundance ^[38]. In addition to investigating
289 cooccurring changes in protein synthesis and abundance, the future use of MSR rather than FSR may
290 allow for new insight by linking changes in ABD to synthesis rates and give a clearer indication of the
291 stoichiometry of multi-protein complexes.

292 In conclusion, the distribution and biological interpretation of protein synthesis data is different when
293 data are expressed as mole synthesis rate (MSR) rather than fractional synthesis rate (FSR). Proteins of
294 low abundance may be ranked amongst the highest in FSR. Therefore, estimation of MSR provides
295 additional insight in experiments where adaptation involves changes to both the abundance and
296 synthesis rate of proteins. In addition, MSR facilitates investigation of changes to the allocation of
297 cellular resources and an indication of which proteins are being synthesised to the greatest extent.
298 Mole synthesis data is largely unreported but as dynamic proteome profiling methods continue to
299 evolve there is potential to gain additional mechanistic insight using MSR measurements. Mole
300 synthesis data may provide new insight to disparities between mRNA and protein abundance
301 measurements as well as support or dispel theories regarding whether components of multi-protein
302 complexes are synthesised in excess.

303 **4. Conflict of interest statement**

304 The authors have declared no conflict of interest.

References

- 305
306
307 [1] S. M. Abmayr, G. K. Pavlath, *Development* 2012, 139, 641.
308 [2] R. M. Cramer, H. Langberg, P. Magnusson, C. H. Jensen, H. D. Schrøder, J. L. Olesen, C.
309 Suetta, B. Teisner, M. Kjaer, *J Physiol* 2004, 558, 333.
310 [3] C. K. Smith, 2nd, M. J. Janney, R. E. Allen, *J Cell Physiol* 1994, 159, 379.
311 [4] F. Relaix, P. S. Zammit, *Development* 2012, 139, 2845.
312 [5] T. Kislinger, A. O. Gramolini, Y. Pan, K. Rahman, D. H. MacLennan, A. Emili, *Mol Cell*
313 *Proteomics* 2005, 4, 887.
314 [6] R. B. Devlin, C. P. Emerson, Jr., *Cell* 1978, 13, 599.
315 [7] N. S. Tannu, V. K. Rao, R. M. Chaudhary, F. Giorgianni, A. E. Saeed, Y. Gao, R. Raghoebar, *Mol*
316 *Cell Proteomics* 2004, 3, 1065.
317 [8] A. F. Millan-Cubillo, M. Martin-Perez, A. Ibarz, J. Fernandez-Borras, J. Gutierrez, J. Blasco, *Sci*
318 *Rep* 2019, 9, 14126.
319 [9] S. B. Cambridge, F. Gnad, C. Nguyen, J. L. Bermejo, M. Kruger, M. Mann, *J Proteome Res*
320 2011, 10, 5275.
321 [10] B. F. Miller, C. A. Wolff, F. F. Peelor, 3rd, P. D. Shipman, K. L. Hamilton, *J Appl Physiol* (1985)
322 2015, 118, 655.
323 [11] V. C. Foletta, M. Palmieri, J. Kloehn, S. Mason, S. F. Previs, M. J. McConville, O. M. Sieber, C.
324 R. Bruce, G. M. Kowalski, *Metabolites* 2016, 6.
325 [12] S. Hesketh, K. Srisawat, H. Sutherland, J. Jarvis, J. Burniston, *Proteomes* 2016, 4, 12.
326 [13] S. J. Hesketh, H. Sutherland, P. J. Lisboa, J. C. Jarvis, J. G. Burniston, *The FASEB Journal* 2020,
327 n/a.
328 [14] D. M. Camera, J. G. Burniston, M. A. Pogson, W. J. Smiles, J. A. Hawley, *Faseb j* 2017, 31,
329 5478.
330 [15] K. Srisawat, K. Hesketh, M. Cocks, J. Strauss, B. J. Edwards, P. J. Lisboa, S. Shepherd, J. G.
331 Burniston, *PROTEOMICS* 2019, n/a, 1900194.
332 [16] J. G. Burniston, Y.-W. Chen, *Omics Approaches to Understanding Muscle Biology*, Springer,
333 2019.
334 [17] L. Li, C. J. Nelson, C. Solheim, J. Whelan, A. H. Millar, *Molecular & cellular proteomics : MCP*
335 2012, 11, M111.010025.
336 [18] C. Gerner, S. Vejda, D. Gelbmann, E. Bayer, J. Gotzmann, R. Schulte-Hermann, W. Mikulits,
337 *Molecular & cellular proteomics : MCP* 2002, 1, 528.
338 [19] K. J. Sollanek, J. G. Burniston, A. N. Kavazis, A. B. Morton, M. P. Wiggs, B. Ahn, A. J. Smuder,
339 S. K. Powers, *PloS one* 2017, 12, e0171007; Z. A. Malik, J. N. Cobley, J. P. Morton, G. L. Close, B. J.
340 Edwards, L. G. Koch, S. L. Britton, J. G. Burniston, *Proteomes* 2013, 1, 290; J. G. Burniston, J.
341 Connolly, H. Kainulainen, S. L. Britton, L. G. Koch, *PROTEOMICS* 2014, 14, 2339.
342 [20] J. C. Silva, M. V. Gorenstein, G. Z. Li, J. P. Vissers, S. J. Geromanos, *Mol Cell Proteomics* 2006,
343 5, 144.
344 [21] C. A. Stead, S. J. Hesketh, S. Bennett, H. Sutherland, J. C. Jarvis, P. J. Lisboa, J. G. Burniston,
345 *Proteomes* 2020, 8.
346 [22] A. J. Holmes, P. J. Rayner, M. J. Cowley, G. G. R. Green, A. C. Whitwood, S. B. Duckett, *Dalton*
347 *Trans* 2015, 44, 1077.
348 [23] J. D. Storey, R. Tibshirani, *Proceedings of the National Academy of Sciences* 2003, 100, 9440.
349 [24] J. Cox, M. Mann, *BMC Bioinformatics* 2012, 13 Suppl 16, S12.
350 [25] E. de Klerk, I. F. Fokkema, K. A. Thiadens, J. J. Goeman, M. Palmblad, J. T. den Dunnen, M.
351 von Lindern, P. A. t Hoen, *Nucleic Acids Res* 2015, 43, 4408.
352 [26] S. Tyanova, T. Temu, P. Sinitcyn, A. Carlson, M. Y. Hein, T. Geiger, M. Mann, J. Cox, *Nature*
353 *Methods* 2016, 13, 731.
354 [27] D. Szklarczyk, A. L. Gable, D. Lyon, A. Junge, S. Wyder, J. Huerta-Cepas, M. Simonovic, N. T.
355 Doncheva, J. H. Morris, P. Bork, L. J. Jensen, C. V. Mering, *Nucleic Acids Res* 2019, 47, D607.

- 356 [28] A. Harada, Y. Ohkawa, A. N. Imbalzano, *Semin Cell Dev Biol* 2017, 72, 77.
- 357 [29] K. A. Carey, D. Segal, R. Klein, A. Sanigorski, K. Walder, G. R. Collier, D. Cameron-Smith,
358 *Pathology International* 2006, 56, 246.
- 359 [30] S. Kumari, S. Roy, P. Singh, S. L. Singla-Pareek, A. Pareek, *Plant Signal Behav* 2013, 8, e22734.
- 360 [31] S. K. Calderwood, A. Murshid, T. Prince, *Gerontology* 2009, 55, 550.
- 361 [32] N. Khurana, S. Bhattacharyya, *Front Oncol* 2015, 5, 100.
- 362 [33] Y. Feng, Z.-M. Tian, M.-X. Wan, Z.-B. Zheng, *World J Gastroenterol* 2007, 13, 2608.
- 363 [34] L. Liu, T. H. Cheung, G. W. Charville, B. M. Hurgo, T. Leavitt, J. Shih, A. Brunet, T. A. Rando,
364 *Cell Rep* 2013, 4, 189.
- 365 [35] A. Fathi, M. Pakzad, A. Taei, T. C. Brink, L. Pirhaji, G. Ruiz, M. Sharif Tabe Bordbar, H.
366 Gourabi, J. Adjaye, H. Baharvand, G. Hosseini Salekdeh, *PROTEOMICS* 2009, 9, 4859.
- 367 [36] V. Andrés, K. Walsh, *J Cell Biol* 1996, 132, 657.
- 368 [37] M. Martin-Perez, J. Villén, *Cell Syst* 2017, 5, 283.
- 369 [38] A. R. Kristensen, J. Gsponer, L. J. Foster, *Mol Syst Biol* 2013, 9, 689.
- 370 [39] S. E. Kruse, P. P. Karunadharm, N. Basisty, R. Johnson, R. P. Beyer, M. J. MacCoss, P. S.
371 Rabinovitch, D. J. Marcinek, *Aging Cell* 2016, 15, 89.
- 372 [40] D. E. Hammond, A. J. Claydon, D. M. Simpson, D. Edward, P. Stockley, J. L. Hurst, R. J.
373 Beynon, *Mol Cell Proteomics* 2016, 15, 1204.
- 374 [41] J. W. Sanger, P. Chowrashi, N. C. Shaner, S. Spalthoff, J. Wang, N. L. Freeman, J. M. Sanger,
375 *Clin Orthop Relat Res* 2002, S153.

377 Figure Legends

378 Figure 1 – C2C12 morphology and mass spectra at different stages of differentiation.

379 Representative light micrograph images of undifferentiated C2C12 myoblasts (0 h; A), and
380 multinucleated myotubes grown without (96 H₂O; B) or with (96 h D₂O; C) heavy isotope label. Density
381 plots of myotube length (D), diameter (E) and area (F) at 96 h in control (red) and labelled (blue)
382 cultures. Mass spectra of peptide [M+2H]²⁺ 894.4711 *m/z* TITLEVEPSDTIENVK (residues 12-27) of
383 ubiquitin-40S ribosomal protein S27a (RS27A) from undifferentiated C2C12 myoblasts (0 h; G), and
384 multinucleated myotubes grown without (96 H₂O; H) or with (96 h D₂O; I) heavy isotope label. Changes
385 in the fraction of the monoisotopic peak (*f_{m0}*) were used to calculate synthesis rates (see Equation 2).

386 Figure 2 – Protein abundance changes during differentiation.

387 (A) Volcano plot illustrating Log₂ fold-change in protein abundance in late (72-96 h) compared to early
388 (0-24 h) differentiation. Statistical significance was determined by one-way ANOVA (153 proteins in
389 *n*=3 samples per group). Data points situated to the left and right of the Y axis represent proteins with
390 a greater abundance in either early or late differentiation, respectively. Proteins exhibiting significant
391 (*P*<0.05, FDR < 1%) differences are coloured red and labelled by their UniProt ID. (B) 2D Enrichment^[24]
392 analysis of significant (*P*<0.02) biological process (red), cellular component (green) and molecular
393 function (blue) annotations in the current protein abundance data (*n*=107) that matched with RNA
394 sequencing data reported in de Klerk et al^[25]. (C) Linear regression of protein abundance change and
395 gene expression change data (*n*=107) used to build the 2D enrichment plot. Consistent with (A) positive

396 fold-change values represent a greater protein abundance/ mRNA expression in late compared to early
397 differentiation.

398 Figure 3 – Comparison of mole and fractional synthesis data in C2C12 cells

399 Linear regression analysis (n=115 proteins) of FSR (%/h) and MSR (fmol/h/ug total protein) during early
400 (0-24 h; A) and late (72-96 h; B) differentiation. Differences between early (0-24 h) and late (72-96 h)
401 differentiation in FSR (C) and MSR (D). Labels represent UniProt identifiers.

402 Figure 4 – Predictive value of FSR and MSR data

403 Linear regression of protein abundance during late differentiation and either FSR (A) or MSR (B) during
404 early (0-24 h) differentiation (n=115 proteins). Linear regression of the change in either FSR (C) or MSR
405 (D) during late versus early differentiation against ribosomal profiling data reported in de Klerk et al ^[25].
406 Positive fold-change values represent greater synthesis in late compared to early differentiation and
407 data points of interest are labelled by their UniProt identifier.

408 Figure 5 – Protein-protein interaction networks

409 Protein-protein interaction networks derived from the top 10 proteins ranked by either FSR (A and C)
410 or MSR (B and D) during either early (A and B) or late (C and D) differentiation. Networks were
411 constructed using the search tool for the retrieval of interacting genes/proteins (STRING). Interaction
412 confidence criteria was set to medium (0.4). Nodes are labelled by gene names and line thickness
413 represents the strength of the data supporting each interaction.

414

415

416

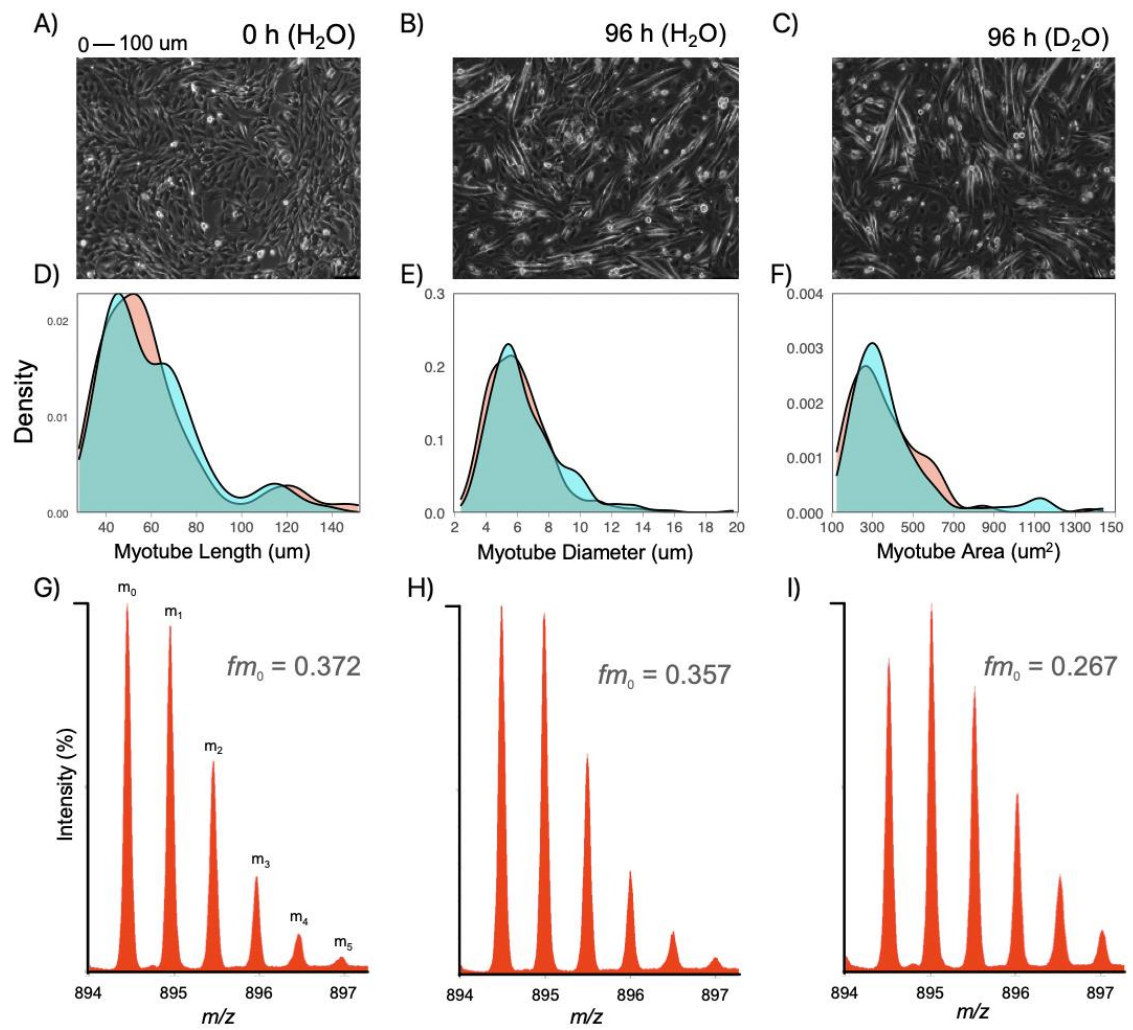
417

418 Figure 1

419

420

Figure 1



422

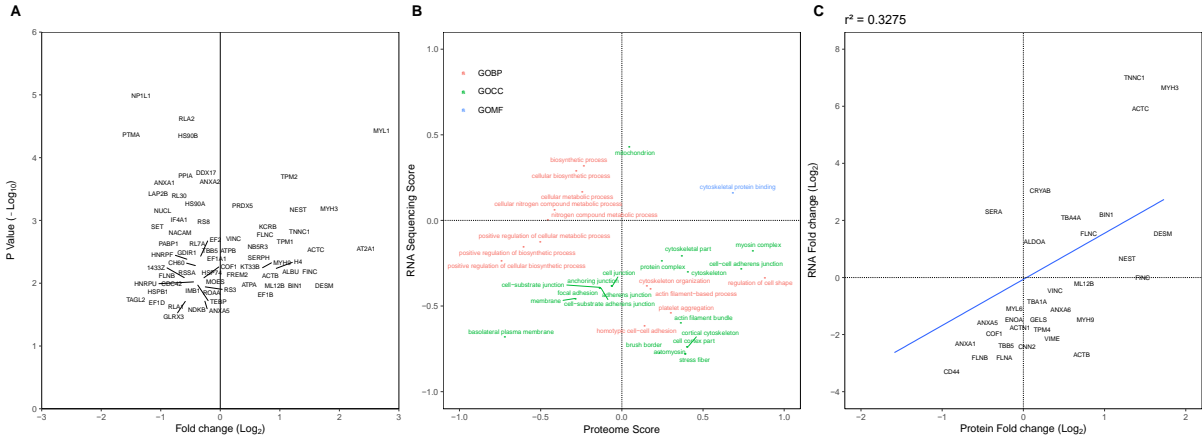
423

424

425

426

Figure 2

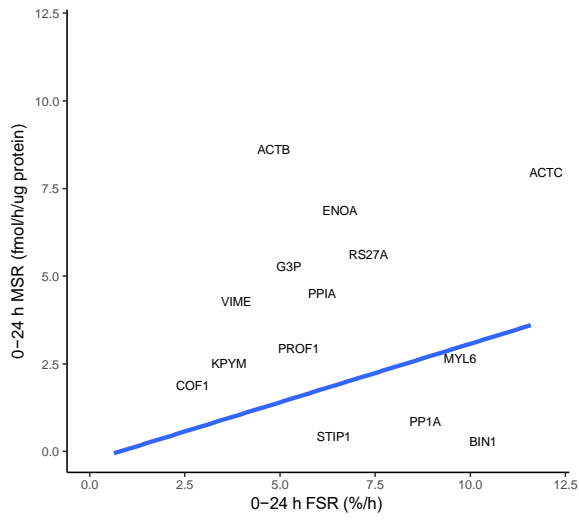


428

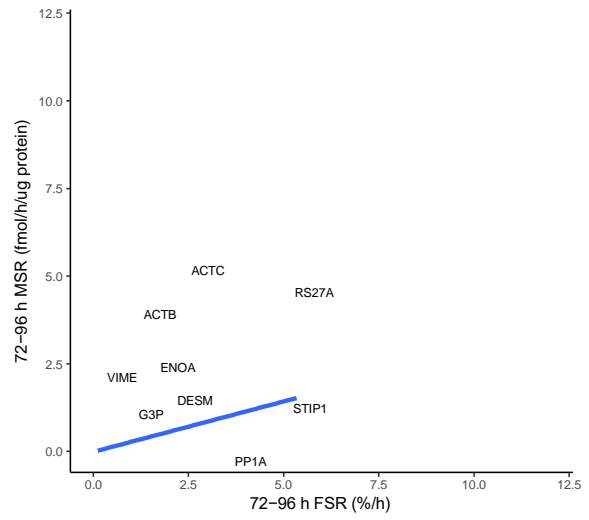
429

Figure 3

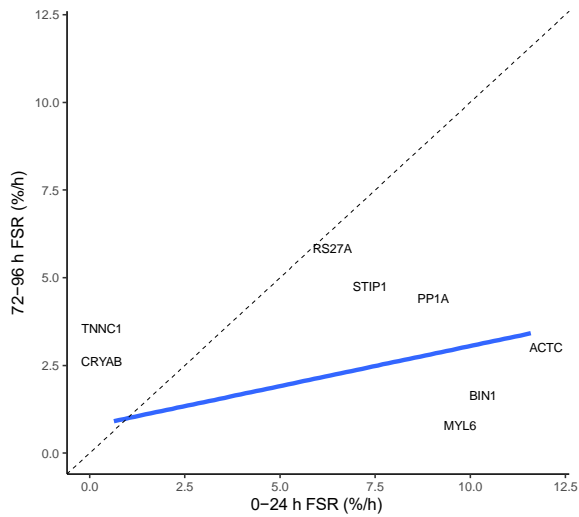
A $r^2 = 0.2040$



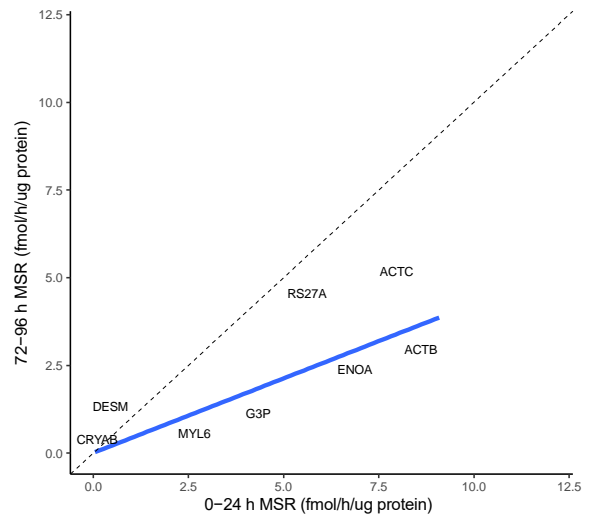
B $r^2 = 0.1652$



C $r^2 = 0.1942$



D $r^2 = 0.7318$

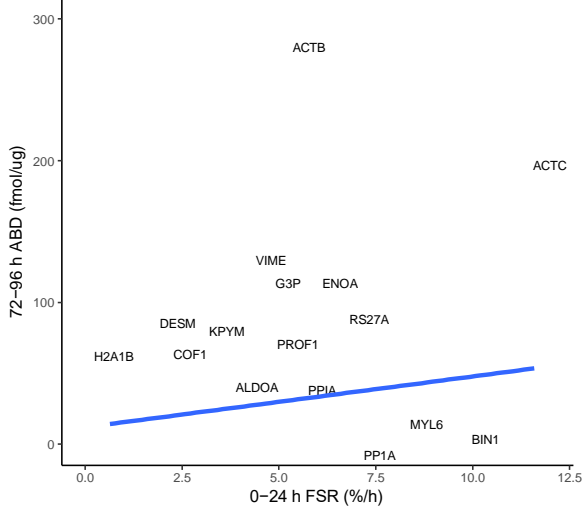


431

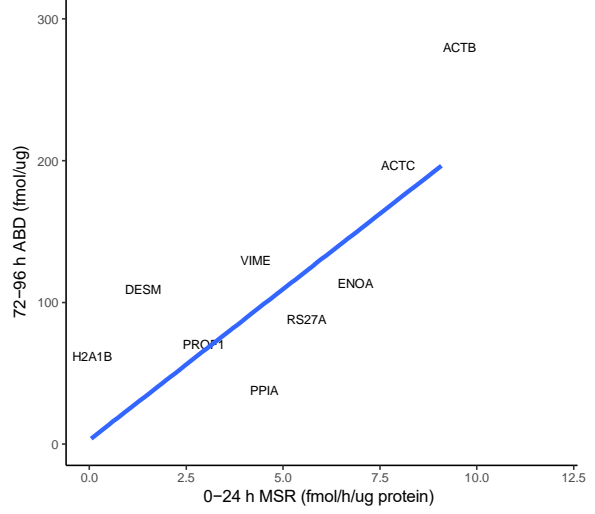
432

Figure 4

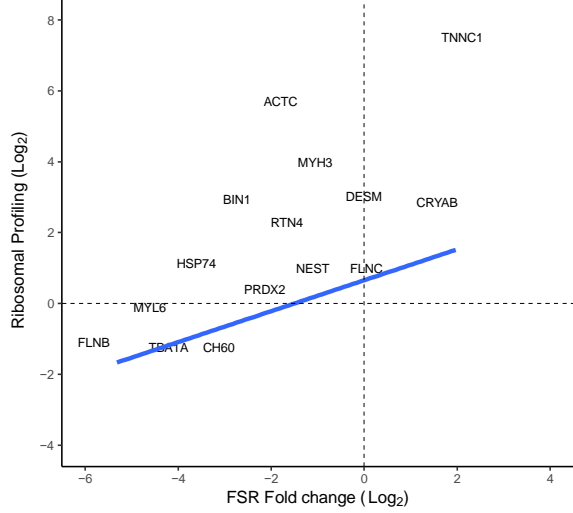
A $r^2 = 0.0405$



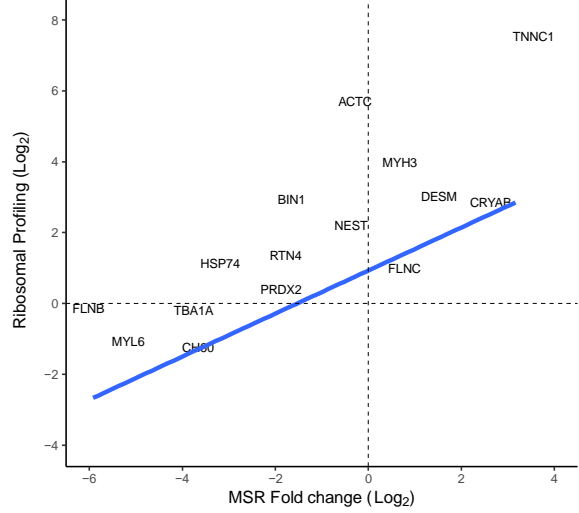
B $r^2 = 0.7790$



C $r^2 = 0.1137$



D $r^2 = 0.2883$

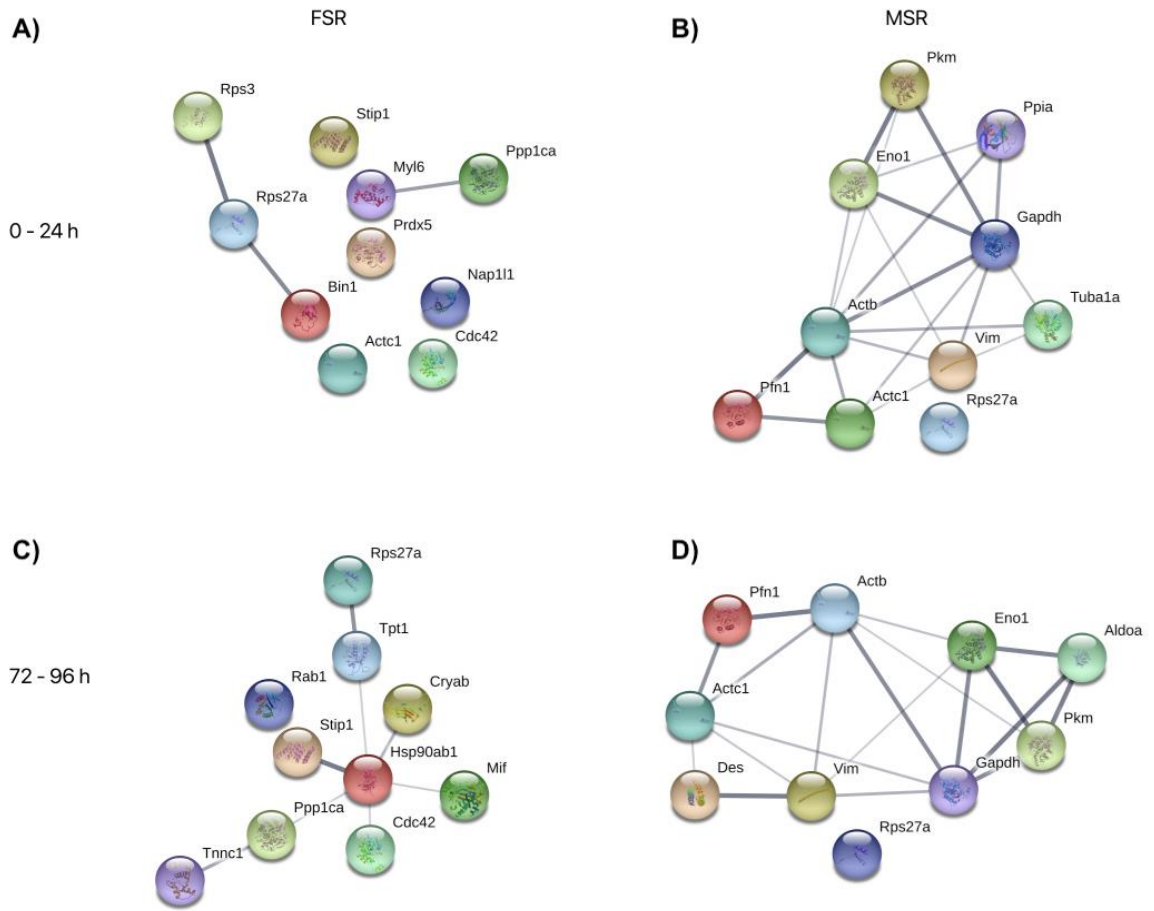


434

435

436

Figure 5



438

439

440